Environ Geochem Health (2026) 48:100
https://doi.org/10.1007/s10653-026-02982-7

ORIGINAL PAPER

Antibiotic mitigation of aqueous systems using untapped potential of unsorted garden waste-derived biochar: performance evaluation and mechanistic insights

Neenu P. Raju · Meenakshi Verma · Pooja Singh · Manikprabhu Dhanorkar

Received: 19 November 2025 / Accepted: 5 January 2026

Abstract The unchecked consumption of antibiotics leads to the persistence of their active form residues in the environment, perpetuating the cycle of exposure, selection and re-infection, which ultimately exacerbates the environmental antimicrobial resistance (AMR). This work aims to provide a direct comparison of different heterogeneous and underutilised biomass as antibiotic adsorbents. This study investigates the adsorption of the antibiotic, specifically Ciprofloxacin (CIP), by biochars produced from two underutilised biomass sources—unsorted Garden waste (GW) and Cashew nut shells (CNS)-at different temperatures (500–700 °C) and residence times (1–2 h). Based on initial adsorption screening and thermogravimetry, GW biochar, produced at 700 °C with a 2-h residence time (GW700 °C/2 h), was selected as the most suitable. A detailed analysis of this biochar was carried out: TGA confirmed the thermal stability; proximate analysis confirmed a high fixed carbon content; BET analysis (59.11 m^2 g^{-1}), FTIR, and XRD indicated the presence of relevant functional groups, and FE-SEM displayed a porous surface morphology, all of which substantiate the adsorption performance. Furthermore, optimum sorption conditions were determined through batch studies, and 50 mg GW700 °C/2 h biochar was found to remove 85.4% of 5 mg L^{-1} CIP in 285 min at a neutral pH. Kinetic and isotherm data confirmed multilayer chemisorption with a maximum sorption capacity of 6.19 mg g^{-1}. This is the first report exploring unsorted GW biochar as a sustainable solution for antibiotic mitigation, which, in future, can be scaled up to be part of the wastewater treatment systems.

Keywords Adsorption mechanism · Antibiotic pollution · Biochar · Cashew nut shell · Ciprofloxacin · Garden waste

Introduction

The uncontrolled use of antibiotics in the healthcare and agriculture sectors, where incomplete metabolism and inadequate wastewater treatment result in increased concentration of pharmaceuticals, especially antibiotics like ciprofloxacin (CIP), which has a half-life of more than 60 days (Islam et al., 2025). The presence of these antibiotic residues creates a selective pressure on the native microbiome, leading to horizontal gene transfer and the enrichment of antibiotic resistance genes in the microbial population, which can then circulate back to the clinical setting via the food chain and water reuse (Naznine et al., 2025). Parallel to the antibiotic pollution, solid waste

Supplementary Information The online version contains supplementary material available at https://doi.org/10.1007/s10653-026-02982-7.

N. P. Raju · M. Verma · P. Singh · M. Dhanorkar (✉)
Symbiosis Centre for Waste Resource Management, Symbiosis International (Deemed University), Pune, India
e-mail: head@scwrm.siu.edu.in; manikadu@gmail.com

Published online: 16 January 2026

management is a significant concern for both human and environmental health, particularly in developing countries with limited waste management resources. Over the past 50 years, waste generation in Asian countries has increased drastically (Agamuthu & Babel, 2023). According to the South Asia Co-operative Environment Programme (SACEP), South Asia generates approximately 334 million tons of waste annually, of which 57% is organic, and the remainder comprises various other industrial hazardous wastes. India, being the most populous country, generates approximately 0.34 kg of solid waste per capita per day (CPCB, 2016). The recyclable fraction in the generated waste is only 15–20% which is at the lower end of global benchmarks (CPCB, 2025).

The transformation of wastes into value-added products is pivotal in a solid waste management strategy (Wan Mahari et al., 2021). Pyrolysis, a temperature-controlled incineration process for biomass, is a widely adopted technology for processing solid waste, yielding a carbon-rich solid product known as biochar (He et al., 2022). The advocacy for biochar has surged in the past decade, laying one of the cornerstones of the circular bioeconomy (Kumar & Bhattacharya, 2020). The porous nature, high surface area, and presence of multiple functional groups make biochar an effective adsorbent for compounds like antibiotics (Kumar and Bhattacharya, 2020). Moreover, biochar is a noteworthy tool in achieving a circular way of living with net-zero discharge, and forms a critical link in the United Nations' Sustainable Development Goals (SDGs) (SDG 11, target 11.6; indicator 11.6.1).

Garden waste and waste from the cashew nut processing sector are two diverse waste biomasses that are underexplored for the production of biochar. Garden waste and cashew industry waste, while differing in origin—urban green residues vs. agro-industrial by-products—offer complementary characteristics as pyrolysis feedstocks. Garden waste is highly heterogeneous and typically rich in lignocellulosic components (Suarez et al., 2023), while cashew shell waste is rich in lignin and high in fixed carbon and calorific value (Coulibaly et al., 2022). Garden or green waste is generated daily, such as foliage, or periodically from maintenance activities like pruning and weeding of the green areas. Globally, on average, 47 kg of garden waste is generated annually per person (Liu et al., 2022b). A significant volume of the waste generated is deposited in open dumps and landfills, with only a small fraction being processed for composting and other uses. In the absence of a robust segregation system in the waste sector of many developing nations, garden waste is often mixed with pre-existing garbage during the disposal process. Garden waste is highly heterogeneous, depending on the individual plants' physicochemical properties, including varied levels of phenolic polymers (lignin), carbohydrates (cellulose and hemicellulose), minerals, proteins, and acids. The species, developmental stage (maturity), and climatic conditions of a plant all affect its chemical makeup (Langsdorf et al., 2021).

Another sector that generates significant quantities of waste is the cashew nut processing industry. Globally, 3.4 to 4.0 million metric tons of cashew shells are produced annually (Zafeer & Bhat, 2023). The cashew nut processing sector has experienced significant growth, primarily in tropical countries such as Brazil, India, and Vietnam. Cashew nut shells contain around 11.50% cellulose, 7.35% hemicellulose, and 7.45% lignin (Nuithitikul et al., 2020). After extracting cashew nut shell oil for industrial use, the shell waste is mainly used as solid fuel in industries, and the rest is disposed of in dumping grounds and landfills. Burning cashew nut shells contributes to greenhouse gas emissions, mainly CO_2 and CH_4, as well as ash disposal.

Converting waste biomass into biochar, which can then be utilised as a low-cost adsorbent for antibiotics, is the most sustainable and circular way of tackling two problems (Fady et al., 2025). In this investigation, two underutilised biomass sources, garden waste and cashew nut shells, are employed to synthesise biochar for CIP removal. The objectives of this study are: (1) production of biochar from GW and CNS feedstocks at different temperatures and residence times, (2) initial adsorption screening of all the produced biochars against CIP, (3) characterisation of the best-performing biochar through proximate and physicochemical characterisation, and (4) optimisation of sorption conditions and model fitting studies of the selected biochar. However, limited studies explore the slow pyrolysis behaviour of these waste streams. Further, the existing literature does not address the comparison of the adsorption behaviour of biochar from underutilised and heterogeneous biomass, especially with respect to CIP. Moreover, a systematic side-by-side performance evaluation of different biomass under controlled pyrolytic conditions for

antibiotics is largely lacking. This study aims to provide a baseline for demonstrating that locally abundant and low-cost tropical waste biomass, without any preprocessing, can be a robust climate-resilient solution for resource-constrained regions facing waste overload and AMR crises.

Materials and methods

Biomass collection and pyrolysis

Garden Waste (GW) and Cashew Nut Shells (CNS) were procured from Symbiosis International (Deemed University), Pune and a Cashew processing unit in Sangli, Maharashtra, respectively. The two feedstocks were thoroughly washed, sun-dried for 24 h, and then oven-dried at 65 °C for 24–48 h. They were subsequently mechanically shredded to yield dry particles of size less than 2 mm (Fig. 1). GW and CNS dry biomass (20 g each) were pyrolysed in a muffle furnace (Bio-Technics India, BTI-36) at a temperature of 500–700 °C for 1–2 h of residence time with an average heating rate of 9.8 °C min^{-1}.

Initial screening of biochars

Adsorption behaviour

Ciprofloxacin (CIP), a member of the Fluoroquinolone class of antibiotics, was selected for the preliminary adsorption studies. Standard curve of CIP was developed using 2.5–60 mg L^{-1} solutions of CIP in 0.01 M $CaCl_2$ (Chemtai et al., 2024). Absorbance was read at 275 nm (Chemtai et al., 2024). A double-beam spectrophotometer (Electronic India, EI-3375) was used to prepare a standard curve. For the batch adsorption screening study, 30 mg of biochar, obtained under different pyrolysis conditions, and a 5 mg L^{-1} CIP solution were used. The reaction mixture was incubated in a shaker incubator (i-therm BTI-05A) at room temperature for 24 h at 100 rpm. Based on the absorbance at 275 nm, the percentage of CIP removal was calculated using Eq. (1).

$$\textit{Removal percent}\,(\%) = \frac{\textit{Initial concentration} - \textit{final concentration}}{\textit{Initial concentration}} \times 100 \quad (1)$$

The biochar giving the maximum CIP removal percentage was selected as the potential adsorbent and taken forward for further characterisation and optimisation studies.

Thermal stability

The thermal stability of CNS and GW biochars was assessed using a thermogravimetric analyser (SETS EVo-TG DTA). Approximately 5 mg of both samples was weighed out in an alumina crucible and heated from room temperature to 900 °C under an air atmosphere with a heating rate of 10 °C per minute. The thermographs generated in OriginPro

Fig. 1 Biomass collection and processing for biochar production. **a** Garden waste **b** Cashew nutshells

software were used to assess the mass loss behaviour of both the biochars and thereby the stability (Meysami et al., 2025).

Characterisation of biochar

The biochar with the highest CIP removal (%) was subjected to various physiochemical characterisations, including proximate analysis, pH, bulk density, and electrical conductivity. ASTM D3172 protocol (ASTM, 2013) was followed for proximate analysis, which included moisture content (MC), volatile matter content (VC), and ash content (AC).

For moisture content, 5 g of the biochar sample was placed in a clean, dry and pre-weighed porcelain crucible and dried in a Hot Air Oven (105 ± 3 °C) for 2 h. Crucibles with biochar were allowed to cool in a desiccator and weighed till a constant weight was reached. The difference between the pre- and post-drying weight of the crucibles was used to calculate MC (%). A completely cooled sample from the MC analysis was placed in a muffle furnace at 900 °C for 10 min. VC (%) was calculated from the difference between the pre- and post-drying weight of the crucible. For ash content, a similar procedure was followed, and biochar was heated at 700 °C for 2 h. Crucibles were allowed to cool in a desiccator and weighed till a constant weight was reached. The difference between the pre-drying and final post-drying weights of the crucible was used to calculate the AC content (%) in the biochar sample. Subsequently, fixed carbon in the biochar samples was calculated using Eq. (2) (Hadey et al., 2022).

$$Fixed\ Carbon\,(\%) = 100 - (MC\% + VC\% + AC\%) \quad (2)$$

Bulk density was measured by tapping a pre-weighed biochar sample into a graduated cylinder and applying Eq. (3) (Khater et al., 2024).

$$Bulk\ density = \frac{Mass\ of\ biochar}{Bulk\ Volume\ of\ biochar} \quad (3)$$

pH and conductivity were measured in a pH meter (Hanna Instruments, HI2221) and a conductivity meter (Hanna Instruments, H14321) using biochar–deionised water suspension (1:10 w/v) (Singh et al., 2017). The selected biochar was characterised using density functional theory (DFT) and the Brunauer–Emmett–Teller (BET) method for surface area determination. The surface area was determined after a 2-h degassing at 120 °C. Additionally, Scanning Electron Microscopy (SEM), Fourier Transform Infrared Spectroscopy (FTIR), and X-ray diffraction (XRD) were also carried out. Surface functional groups were identified using FTIR (Bruker ALPHA II) across the range of 400–4000 cm^{-1}, with analysis performed in R software, version 12.1 + 563, 2024. Surface morphology of the selected biochar was assessed using FE-SEM (FEI Nova NanoSEM 450), and structural analysis was done through Rigaku Miniflex 600 X-Ray Diffractometer (Lewczuk et al. 2021).

Influence of adsorption parameters

Garden waste-derived biochar (GW700 °C/2 h), with the highest CIP removal (%) and highest surface area, was subjected to detailed adsorption studies to determine the different factors influencing the adsorption performance.

The adsorbent dosage, pH, and CIP concentration were determined by following Chemtai et al. (2024). Briefly, 50 mL of 0.01 M $CaCl_2$ with 5 mg L^{-1} CIP was treated with varying biochar doses (10–60 mg) at different pH levels (1–14). The optimal dose and pH, once obtained, were then used to test different CIP concentrations (1–50 mg L^{-1} prepared in 0.01 M $CaCl_2$ solution). After 24 h of mixing at 100 rpm, the samples were centrifuged at 7000 rpm for 10 min to remove the biochar particles, and CIP removal was analysed by absorbance at 275 nm (Chemtai et al., 2024).

Batch equilibrium studies were conducted using the optimum dose of biochar in 50 mL of 0.01 M $CaCl_2$ with the optimum CIP concentrations at the optimal pH (Chemtai et al., 2024). To determine the equilibrium contact time, 2 ml of the sample was withdrawn at regular intervals from each CIP concentration till the equilibrium time was reached. The absorbance was measured at 275 nm, and the adsorption equilibria were determined based on removal efficiency over time.

Adsorption models (Isotherms and Kinetics)

The adsorbent-adsorbate interactions were determined using the Langmuir equation [Eq. (4) & Eq. (5)] and the Freundlich, Eq. (6) models (Murphy et al., 2023).

$$q_e = \frac{q_{max}.K_L.C_e}{1 + K_L.C_e} \tag{4}$$

$$R_L = \frac{1}{C^0 + K_L} \tag{5}$$

$$q_e = K_F.C_e^{\,1/n} \tag{6}$$

The data generated was fitted into Pseudo-First Order (PFO) and Pseudo-Second Order (PSO) kinetic models. Equations (7) and (8) describe the linear equations for PFO and PSO, respectively (Murphy et al., 2023).

$$\ln(q_e - q_t) = lnq_e - lnk_1 t \tag{7}$$

where q_e and q_t are the adsorption capacities (mg g^{-1}) at equilibrium and time t, and k_1 is the rate constant (min^{-1}).

$$\frac{t}{q_t} = \frac{1}{k_2 q_{e2}} + \frac{1}{q_e} t \tag{8}$$

where k_2 is the rate constant (g mg^{-1} min^{-1}), and q_e, q_t are defined above.

Results and discussion

Biomass collection and pyrolysis

The yield of biochar is significantly influenced by pyrolysis temperature, residence time, and the type of parent feedstock. The importance of pyrolysis conditions was evident in the current work, where pyrolysis of GW at 550 °C and 700 °C yielded 62% and 55% biochar, respectively (Supplementary Tables 1a, 1b). The biochar yield from the pyrolysis of CNS biomass at 500 °C was 20.47%, reiterating the significant role played by the feedstock. An increase in temperature caused a decrease in the yield, and the lowest biochar yield was observed for CNS at 700 °C with 1 h residence time (16.43%). This result is consistent with earlier work, which has well established the dependency of biochar yield on feedstock properties, pyrolysis conditions, and heating rate (Khater et al., 2024). Higher temperatures and longer residence durations typically reduce the yield due to greater volatile loss. The feedstock composition and pyrolysis temperatures play a key role in the quality of biochar. Generally, the feedstock composition determines the porosity of the biochar, while the pyrolysis temperature influences the structural stability and surface chemistry (Xuan & Phuong, 2024). This is well evident from the difference in the yield of GW and CNS biochars.

Initial screening of biochars

Adsorption behaviour

A standard curve for CIP with R^2 of 0.9935 (Supplementary Fig. 1) was established. Equation (9) was generated from the standard curve and used for all subsequent adsorption calculations (Chemtai et al., 2024).

$$y = 0.064x + 0.0345 \tag{9}$$

The initial adsorption study of all the biochars produced revealed that the CIP removal percentage of CNS biochar was minimal (0–7%), with CNS 600 °C/1 h showing no adsorption activity and 700 °C/1 h CNS-biochar showing the highest (7.1%). In contrast, GW biochars obtained with a residence time of 1 h had low CIP removal activity (< 10%). However, GW biochar obtained at a 2-h residence time at pyrolysis temperatures of 550, 650, and 700 °C showed significantly higher CIP removal, at 32.4%, 53.1%, and 72.7%, respectively (Supplementary Fig. 2).

The observed poor performance of CNS-biochar can be attributed to its chemical composition and overlapping absorbance with CIP. Araújo et al. (2023) studied in detail the behaviour of different compounds in the CNS and found that some of the compounds (cardinol derivatives) have absorption maxima around 270–280 nm. The absorption maxima of CIP are also at 275 nm; hence, it was proposed that the overlap between the absorbance spectra of CIP and CNS-derived compounds can hinder accurate spectrophotometric measurements. For GW biochars, higher temperatures and longer pyrolysis

times enhanced porosity through possible devolatilization of lignin and cellulose, thereby improving the adsorption capacity of biochar produced at higher pyrolysis temperatures (Qiu et al., 2023). Thus, GW biochar produced at 700 °C with a 2-h residence time (GW700 °C/2 h) was selected for further in-depth characterisation and adsorption studies.

Thermal stability

The TGA of CNS and GW biochar in air up to 900 °C revealed a typical three-stage lignocellulosic decomposition (Ma et al., 2019). There is an initial dehydration up to 200 °C, followed by active devolatilization between 200 °C and 500 °C, and finally, slow oxidation at higher temperatures (Ma et al., 2019). The thermograph (Fig. 2) of CNS biochar shows a major weight loss between 250 and 500 °C, which can be attributed to the overlapping degradation of hemicellulose and cellulose, whose decomposition windows have been widely reported to be within 200–315 °C and 315–400 °C, respectively (Fatmawati et al., 2023). In contrast, the GW biochar exhibited a multistep devolatilization process, with a high solid residue remaining at 900 °C. This indicates the higher content of lignin, which is known to decompose over an extended temperature range (200–600 °C), enhancing the yield (Panizio et al., 2024). Overall, GW biochar was more thermally stable than CNS, as it was substantiated by the yield and surface chemistry.

Characterisation of GW biochar

Pyrolysis temperature and residence time play crucial roles in determining the surface characteristics of the resultant biochar. An increase in temperature leads to an increase in the release of volatile matter, resulting in enhanced surface pores, as also reported in earlier studies (Handiso et al., 2024). Moreover, the increase in residence time prolongs the pore formation process due to enhanced devolatilization and the development of a network of mesopores and micropores (Handiso et al., 2024). BET analysis of GW-biochar in the current study corroborated these findings. The highest surface area (59.11 $m^2\ g^{-1}$) was obtained for GW700 °C/2 h biochar as compared to all other GW biochars assessed (Supplementary Table 2). Biochar obtained was alkaline in nature (pH 8.9) with 76.37% fixed carbon content (Table 1).

The physicochemical properties of GW at 700 °C/2 h confirm its suitability for adsorption processes and environmental applications. The low moisture content (1.37%) and volatile content (7.86%) indicate effective devolatilization and enhanced biochar stability, in line with previous studies (Handiso et al., 2024). A high fixed carbon content (76.37%) suggests strong carbon sequestration potential and long-term stability, further substantiated by Lehmann and Joseph (2016). The alkaline pH (8.93) is ideal for neutralising acidic soils, while the moderate bulk density (0.86 g cm^{-3}) supports practical handling. The low electrical conductivity (0.045 µS) indicates minimal soluble

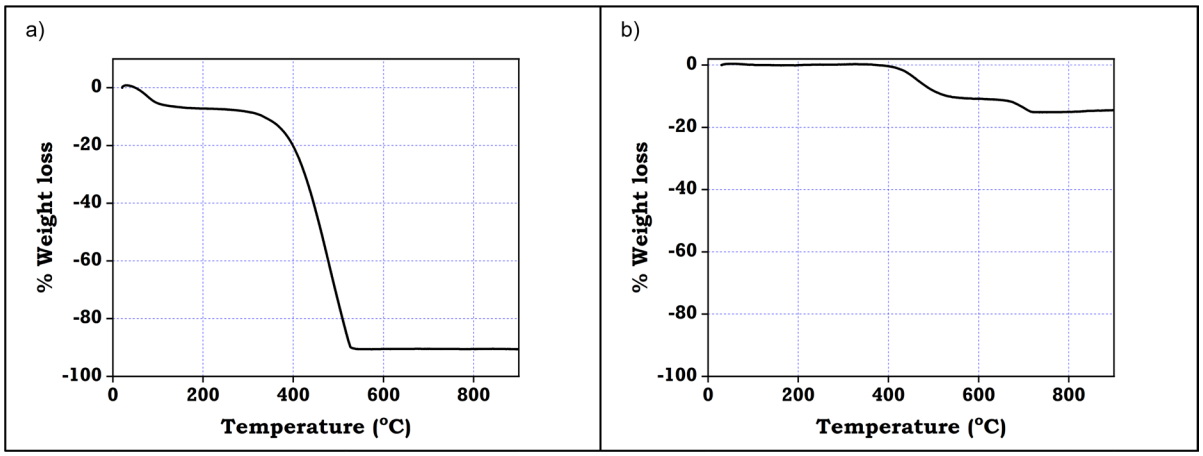

Fig. 2 TGA thermograph of **a** CNS biochar, and **b** GW biochar

Table 1 Physicochemical characterisation of GW700°C/2 h biochar

Sr. No:	Parameter	GW700°C/2 h
1	BET Surface Area ($m^2\ g^{-1}$)	59.11
2	Pore Volume (cc g^{-1})	0.05
3	Pore density (nm)	3.79
4	MC %	1.37 ± 0.15
5	VC %	7.86 ± 1.06
6	AC %	14.4 ± 0.75
7	FC %	76.37 ± 1.69
8	pH	8.93 ± 0.04
9	Bulk density (g m^{-3})	0.87 ± 0.02
10	Electrical conductivity (µS)	0.05 ± 0.07

salts, thereby reducing salinity risks in agriculture and the need for additional salt inputs during water treatment. These characteristics align with the properties of typical high-temperature biochars, establishing GW700 °C/2 h as a conducive material for multi-functional environmental applications, such as pollutant adsorption, carbon sequestration, and soil amendment (Haider et al., 2022).

Surface structure, morphology and functional group characterisation.

Structural and physicochemical characterisation of GW700 °C/2 h biochar revealed that the biochar with the highest surface area (GW700 °C/2 h) exhibited the lowest pore volume (0.05 cc g^{-1}), while having a larger average pore size (3.79 nm). This suggests that during high-temperature pyrolysis, the average pore size can increase due to the coalescence and widening of existing pores, while the total pore volume may decline due to structural collapse and ash-induced blockage (Edeh et al., 2023). This trend is consistent with the findings of previous studies, which have reported an increase in average pore size with increasing pyrolysis severity (Jawad et al., 2021). The larger the surface area and the wider the pores, the more critical they are for enhancing the CIP adsorption. In the initial screening study, GW700 °C/2 h showed the highest CIP removal percentage, which can be attributed to the high surface area and pore size, as also reported by Blachnio et al. (2023).

The XRD analysis of GW700 °C/2 h biochar revealed a predominantly amorphous carbon structure, as evident from the broad hump between 15° and 25°angle, which is typical of disordered carbon formed during high-temperature pyrolysis. Superimposed sharp peaks indicate the presence of crystalline minerals such as quartz (26.5°), potassium, calcite, hydroxyapatite (28.5°–31.8°), alkali salts like KCl and NaCl (39.5°–42°), iron oxides (~45.5°), and aluminosilicates (~50.2°), confirming the incorporation of thermally stable inorganic components (Lewczuk et al., 2021; Fig. 3).

FTIR spectroscopy further identifies and confirms the presence of key functional groups. A broad band around 3360 cm^{-1} corresponds to O–H stretching (alcohols, phenols, or acids) while the peak at 2904 cm^{-1} relates to C–H bonds. The small peak at 1797 cm^{-1} indicates C=O stretch, and a prominent peak at 1024 cm^{-1} is indicative of C–O stretch. The fingerprint region (below 1000 cm^{-1}) exhibited multiple bands, indicating complex molecular vibrations (Fig. 2b). FE-SEM images revealed irregularly shaped biochar particles with rough surfaces and agglomeration at lower magnification (50,000x). Higher magnification (100,000x) revealed a network of interconnected pores and granular textures (Fig. 2c). This porous structure is crucial for enhancing surface area and adsorbate accessibility, and is essential for applications such as adsorption, catalysis, and soil amendment (Lewczuk et al., 2021).

The structural characterisation of GW700 °C/2 h biochar highlighted its suitability for adsorption applications. Characterisation via XRD indicated the presence of a predominantly amorphous carbon matrix intertwined with crystalline quartz, calcite, and feldspar mineral inclusions, which is characteristic of biochars generated under high-temperature pyrolysis conditions, as asserted by Pusceddu et al. (2019). Incorporating these minerals enhances ion exchange and surface reactivity. Furthermore, FTIR confirmed the presence of functional groups comprising hydroxyl, carbonyl, and C-O bonds, which are instrumental in mediating adsorption processes through hydrogen bonding and electrostatic interactions (Liu et al., 2022a). FE-SEM imaging revealed a complex, porous framework with a heterogeneous external morphology, consistent with prior research by Suman et al. (2017), who correlated high surface topography and pore interconnectivity with enhanced adsorption efficacy. These empirical findings substantiate that biochar's surface chemical properties, porosity, and mineral content significantly contribute

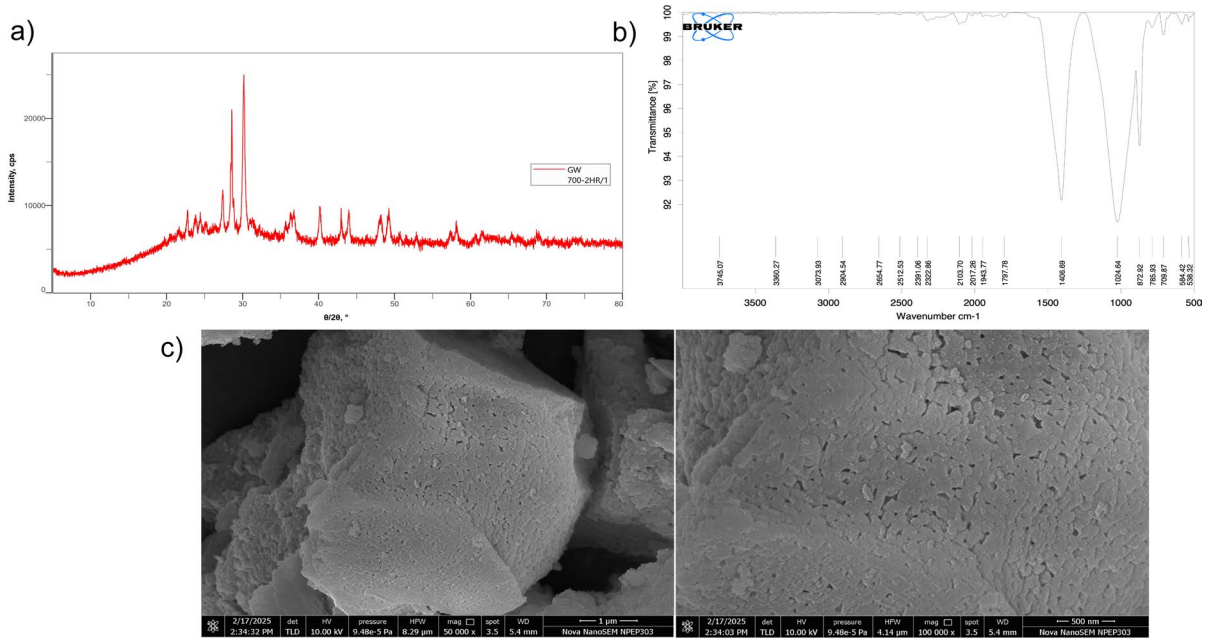

Fig. 3 Surface characterisation of garden waste-derived biochar (GW700 °C/2 h) **a** XRD spectra; **b** FTIR spectra, and **c** FE-SEM image

to its potential as a high-performance adsorbent, particularly for contaminants such as CIP.

Influence of adsorption parameters on GW700 °C/2 h biochar.

A detailed analysis of the adsorption efficiency of GW700 °C/2 h biochar confirmed its superior adsorbing capacity (Fig. 4). According to the analyses, a 50 mg dose of biochar (Fig. 4a) exhibited superior efficacy in removing 5 mg L^{-1} ciprofloxacin (Fig. 4b) at neutral pH (Fig. 4c), achieving a removal efficiency of 85.35%. Subsequently, the equilibrium time and concentration of the batch adsorption system were found to be 285 min and 5 mg L^{-1}, respectively (Fig. 4d; Supplementary Table 3a and 3b).

Determining the optimal adsorbent-adsorbate ratio is crucial, as excessive dosing can compromise the effective surface area due to particle aggregation (Liu et al., 2022b). A neutral pH environment favoured CIP adsorption, possibly by enabling the zwitterionic form, which facilitates electrostatic, hydrogen bonding, and hydrophobic interactions (Shaha et al., 2024). Adsorption equilibrium was established at 285 min, indicating a complex process involving both diffusion and surface binding mechanisms. Notably, the concentration of 5 mgL^{-1} CIP corresponds to environmentally relevant levels, thereby ensuring the practicality of this removal method. These findings align with those of Sowjanya et al. (2023), who found that a CIP concentration of 10–30 mg L^{-1} at near-neutral pH was optimal for adsorption. The equilibrium data supported further adsorption isotherm and kinetic modelling to explore adsorption capacity and mechanisms. Even though the biochar pH was alkaline (pH 8.93), the optimum CIP adsorption was at neutral pH (Fig. 4c). These findings are in alignment with Chauhan et al. (2022), who suggested that the process for adsorption is not solely governed by electrostatic forces but rather by a combination of π–π interaction, hydrogen bonding and electrostatic forces.

Adsorption models (isotherms and kinetics)

The current study explored the Langmuir and the Freundlich models to evaluate the adsorbent-adsorbate interaction and the adsorption capacity. Two models, PFO and PSO, were used to assess the reaction kinetics, which describe the nature of the adsorbent-adsorbate interaction. These models can determine the applicability of the biochar through the adjusted

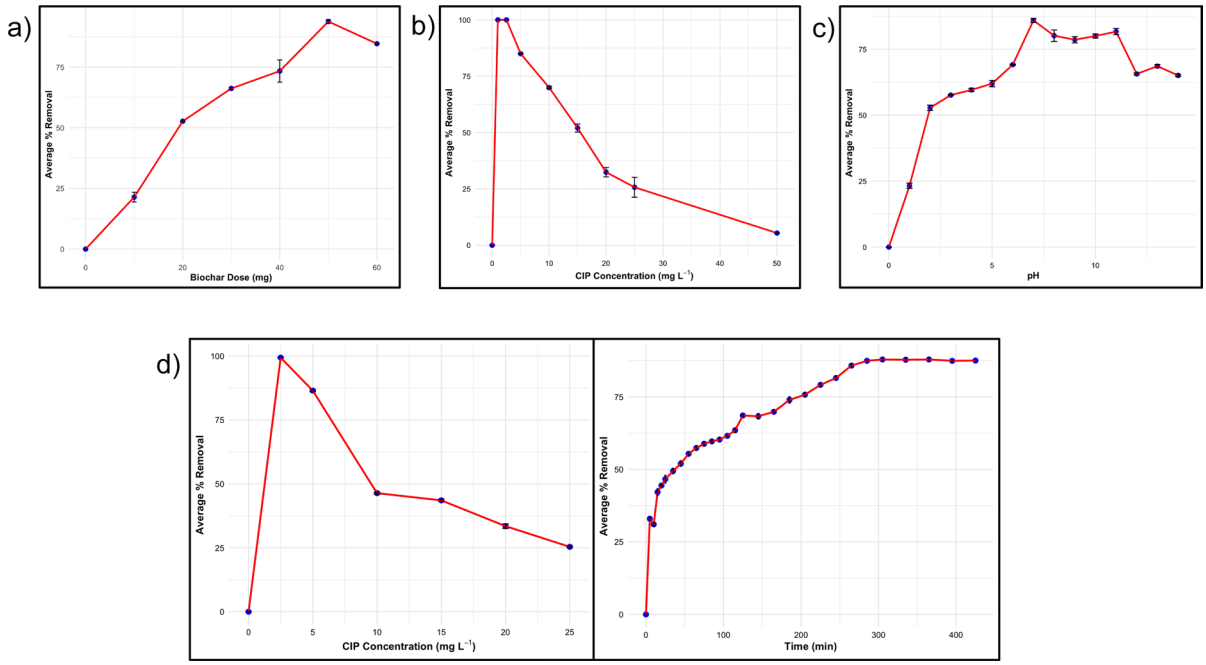

Fig. 4 Optimisation of adsorption conditions: **a** Biochar dose, **b** CIP concentration, **c** pH, and **d** equilibrium time and concentration determination

coefficient of determination (Cavali et al., 2025). The Langmuir model indicates monolayer adsorption on the adsorbent surface, with no further adsorption occurring once a site is occupied (Mirizadeh et al., 2023). The Freundlich model, on the other hand, describes multilayer adsorption on a heterogeneous surface (Mirizadeh et al., 2023). Isotherm analysis of biochar (GW700 °C/2 h) revealed that the Freundlich model ($R^2 = 0.93$) provided a better fit compared to the Langmuir model ($R^2 = 0.87$), indicating that multilayer adsorption on a heterogeneous surface is primarily at play (Table 2).

The Langmuir model ($R^2 = 0.87$) yields qmax = 6.20 mg g^{-1} and a large affinity constant KL = 41.81 L mg^{-1}, while the separation factor RL = 0.00447 lies between 0 and 1 and approaches zero, evidencing highly favourable monolayer adsorption on relatively uniform sites—interpretations that follow standard Langmuir criteria used in water treatment design. Although a lower R^2 showed limited applicability, a high Freundlich n value (6.50)

Table 2 An overview of all model fitting studies performed on GW700°C/2 h biochar

Model		R^2	Key Parameters
Kinetic	Pseudo First Order (PFO)	0.89	K1(rate constant) = 0.02 min^{-1}; $q_e = 3.24$ mg g^{-1}
	Pseudo Second Order(PSO)	0.98	K2 (rate constant) = 0.00624 μg·mg^{-1}·min^{-1} $q_e = 5.14$ mg g^{-1}
Isotherm	Langmuir	0.87	$q_{max} = 6.20$ mg g^{-1} KL = 41.81 RL = 0.00447
	Freundlich	0.93	Kf = 1.95; n = 6.50

confirmed favourable adsorption. These findings align with recent literature recommending the use of advanced models to capture complex adsorption behaviours (Mirizadeh et al., 2023).

The kinetic models describe the rate and nature of the adsorption process. PSO assumes adsorption site availability and not the initial adsorbate concentration to primarily determine the rate, while PFO assumes that the initial concentration of adsorbent and adsorbate are directly proportional (Cavali et al., 2025). The kinetic analysis of CIP adsorption onto GW700 °C/2 h biochar indicated that the pseudo-second-order (PSO) model ($R^2 = 0.98$) better described the process than the pseudo-first-order (PFO) model ($R^2 = 0.89$) (Fig. 4). This was indicative of chemisorption as the dominant mechanism for CIP adsorption. The PSO model predicted q_e (5.14 mg g^{-1}), which closely matched the experimental value (4.61 mg g^{-1}). In contrast, the PFO model underestimated it, suggesting that diffusion played a lesser role, as was also suggested in earlier studies (Cavali et al., 2025). Moreover, the q_{max} (maximum adsorption capacity) of GW700 °C/2 h biochar was found to be 6.19 mg g^{-1} (Fig. 5).

The low Error Sum of Squares Residual (ESSQR) for the Freundlich model (0.01) confirmed its superior fit, indicating heterogeneous adsorption. In contrast, the Langmuir model (ESSQR = 0.11) suggested monolayer adsorption but with lower accuracy. Among kinetic models, the PSO model (ESSQR = 0.28) fits acceptably, highlighting chemisorption, whereas the PFO model (ESSQR = 2.16) poorly represented the process (Supplementary Table 4). These findings, consistent with Simonin (2016), underscore the importance of model selection. Overall, the strong fit of the PSO and Freundlich models suggested

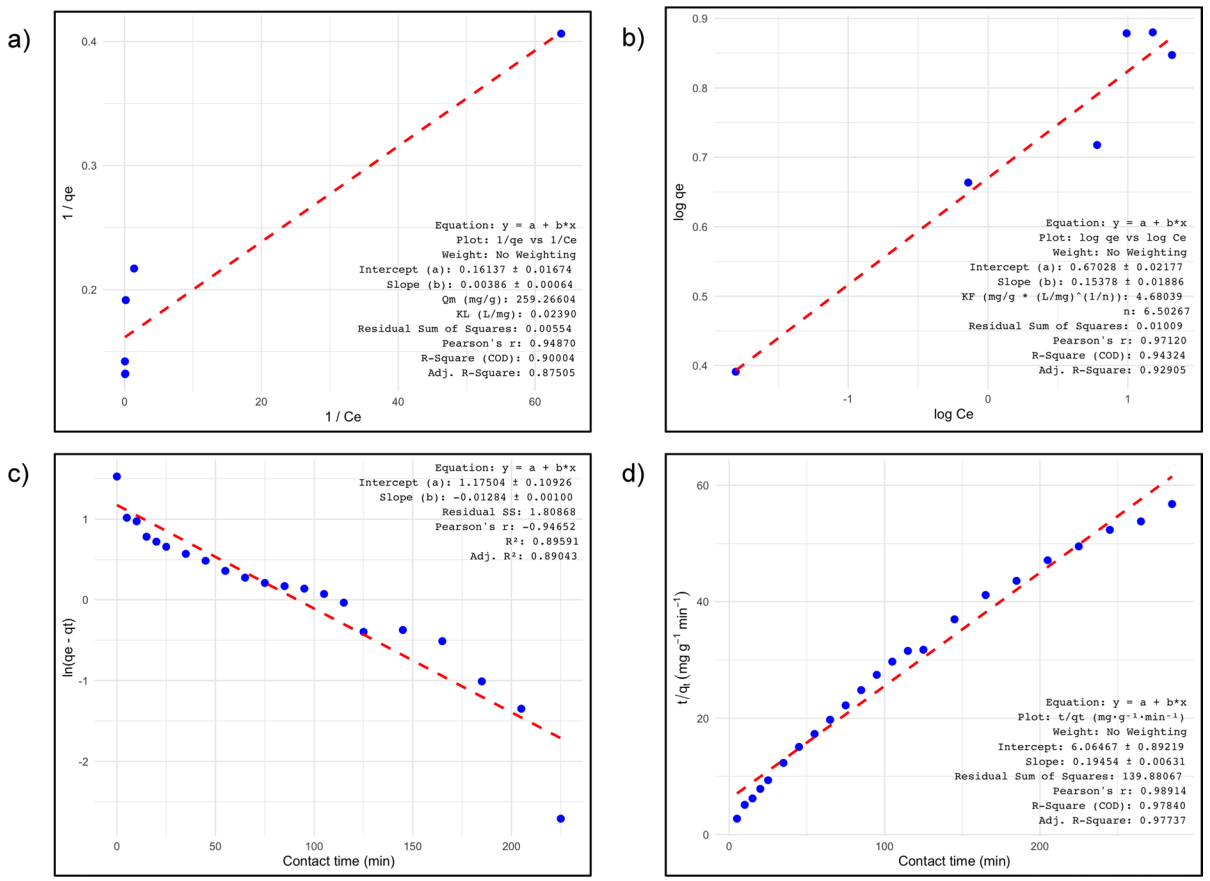

Fig. 5 Adsorption isotherm and kinetic model fitting: **a** Langmuir model, **b** Freundlich model, **c** Pseudo-First Order (PFO) kinetic model, and **d** Pseudo-Second Order (PSO) kinetic model

chemisorption on a heterogeneous surface, with high adsorption capacity and strong CIP-biochar interactions. A consolidated summary of all adsorption parameters is in Table 3.

Comparison of the adsorption behaviour of different garden waste biochars with the current unmodified, 700 °C unsorted garden-waste biochar delivered a BET of 59.11 m^2g^{-1} and a CIP q_{max} of 6.19 mg g^{-1}—appropriate for an amphoteric pharmaceutical removal from aqueous systems. In its pristine form, GW700 °C/2 h exhibits a promising, low-cost, and scalable solution for emerging contaminants, such as antibiotics (Table 4). Even though these modified biochars have a higher sorption capacity, a cost-effective solution favours adsorbents with less secondary waste and a more sustainable production (Wakejo et al., 2022). In this context, the developed GW700 °C/2 h offers a balance between complexity and performance for the effective removal of CIP from an aqueous system.

Mechanistic elucidation of adsorption using characterisation and literature evidence

The detailed characterisation of GW700 °C/2 h revealed a possible mechanism of biochar-CIP interaction. The current study yielded a biochar with a surface area of 59.12 m^2 g^{-1}, pore volume of 0.05 cm^3 g^{-1}, and

Table 3 Summary of optimum adsorption parameters for GW700 °C/2 h

Adsorption Parameters	Optimum Condition	Unit
Biochar dose	50	mg
CIP dose	5	mg L^{-1}
pH	7	-
CIP removal	85.35	%
Equilibrium time	285	minutes
Equilibrium concentration	5	mg L^{-1}
Maximum adsorption capacity (q_{max})	6.19	mg g^{-1}
Adsorption isotherm	Freundlich	–
Kinetic model	Presuo Second Order	–

Table 4 Comparison of the adsorption behaviour of different garden waste-derived biochar

Feedstock/Biochar	Pyrolysis Temperature (°C)	Modified/Unmodified biochar	BET surface area (m^2 g^{-1})	q_{max} (mg g^{-1})	Pollutants removed	References
Six garden-waste biochars	300, 500, 700	Unmodified	Not reported	51.39	Cr (VI)	Zhang et al. (2021)
Garden waste biochar	500–1000	Polyethyleneimine-modified	Not reported	56.1	Cr (VI)	Wei et al. (2025)
Garden waste biochar	800	Polyethyleneimine- and magnetically modified	Not stated	52.6	Cr (VI)	Tie et al. (2025)
Garden-waste biochar	500	Unmodified	Not reported	20.5 (Cs), 25.2 (Cu), 12.4 (Ni), 45.9 (Pb)	Cs^+, Cu^{2+}, Ni^{2+}, Pb^{2+}	Mészáros et al. (2023)
Urban pruning-waste biochar (Wild privet)	400, 500, 700	Unmodified	94.28	13.85 (Pb^{2+}), 5.59 (Cd^{2+}), 28.14 (Mn^{2+})	Pb^{2+}, Cd^{2+}, Mn^{2+}	Abyaneh et al. (2024)
Unsorted Garden Waste Biochar	700	Unmodified	59.12	6.19	Ciprofloxacin	This study

mesopore size ≈of 3.8 nm, all of which point towards a texture that allows a rapid diffusion and intraparticle transport of CIP with minimal to no steric hindrance (Chemtai et al., 2024). The presence of several crystalline phases—calcite/hydroxyapatite, aluminosilicates, quartz, and iron oxides (revealed through XRD)—on the heterogeneous surfaces (revealed through FE-SEM) further accentuated the adsorption spectrum. This finding aligns with the observations of Zhao et al. (2025), who explicitly noted that adsorption is not purely surface-area limited, but rather is influenced by site chemistry and mineral assistance. This was further corroborated by the Freundlich multilayer behaviour across concentrations and the kinetic fit to pseudo-second-order, indicating that the rate-limiting step is dominated by surface interactions after diffusion (Chemtai et al., 2024). Finally, it can be proposed that the alkaline pH of the biochar (8.93) causes the carboxyl group of CIP to deprotonate, making it a substantial oxygen donor and enabling it to bind with metals such as iron (Azzam et al., 2024). Based on this, Fig. 6 elucidates a possible mechanism of CIP removal using GW700 °C/2 h biochar.

Four significant steps are primarily proposed for possible adsorption:

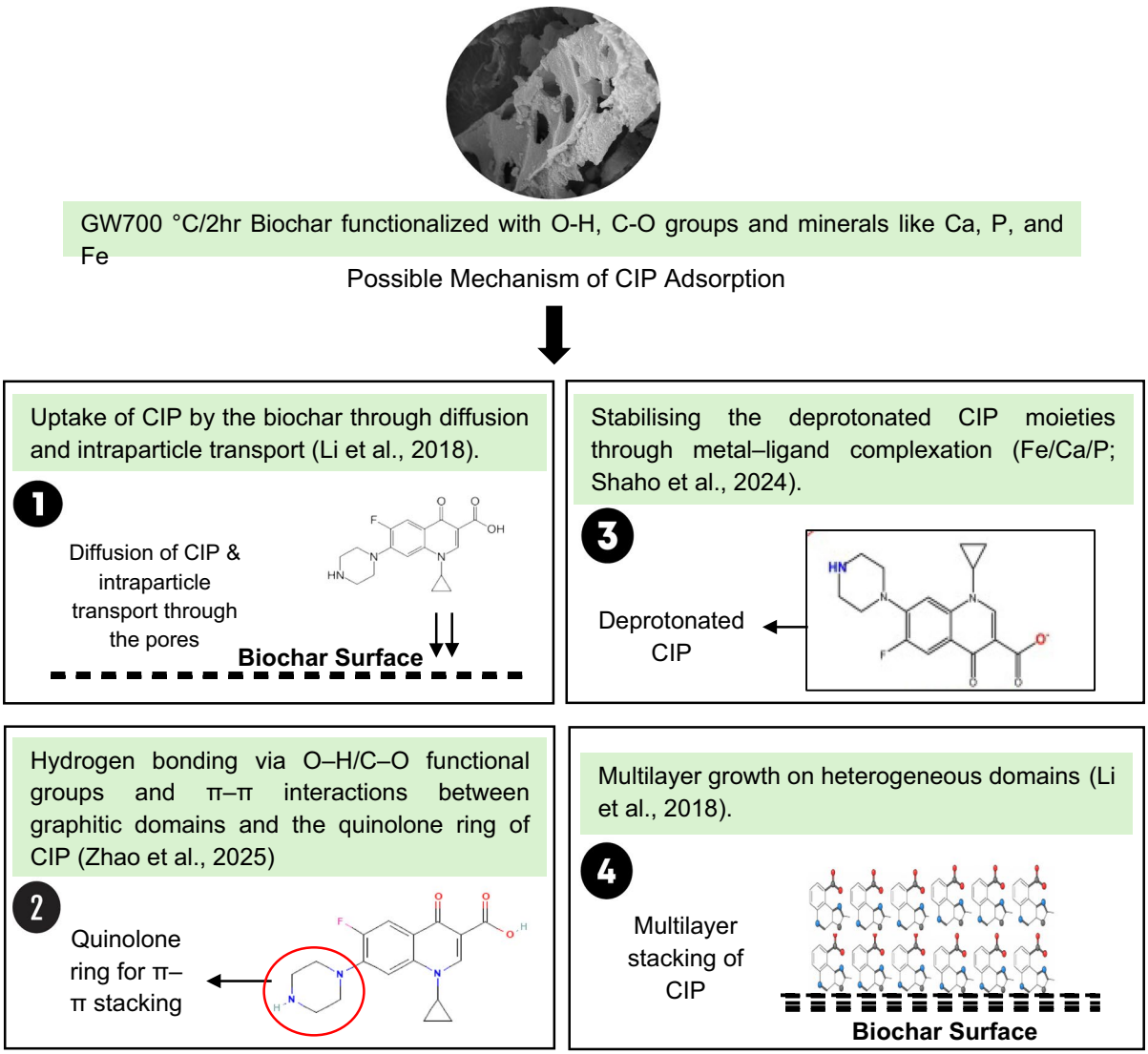

Fig. 6 Possible mechanisms of adsorption of CIP by GW700 °C/2 h biochar

(i) diffusion and intraparticle transport of CIP (Li et al., 2018), (ii) hydrogen bonding via O–H/C–O functional groups and π–π interactions between graphitic domains and the quinolone ring of CIP (Zhao et al., 2025), (iii) stabilising the deprotonated CIP moieties through metal–ligand complexation/bridging at Fe/Ca/P sites and ion exchange (Shaho et al., 2024), and iv) multilayer growth on heterogeneous domains (Li et al., 2018). Thus, despite the moderate BET surface area, the GW700 °C/2 h showed a higher CIP removal efficiency, aligning the structure–function relationships from FTIR/XRD/SEM with the Freundlich-PSO profile.

Conclusion

This study produced the first comparative assessment of unsorted garden waste and cashew nut shells biochars as adsorbents for ciprofloxacin and identified GW700 °C/2 h as the most effective adsorbent, with an removal percentage of 85.35% at neutral pH with maximum adsorption capacity (q_{max}) of 6.19 mg g^{-1}. The superior performance of unmodified GW700 °C/2 h is attributed to its moderate surface area, heterogeneous pore distribution, presence of metals and minerals. With a comprehensive physical, functional and morphological characterisation (TGA, BET, FTIR, XRD, and FE-SEM) and supporting literature evidence, this study proposes a possible adsorption mechanism for GW700 °C/2 h with CIP. The initial bonding of CIP to the adsorbent occurs through π–π interactions and hydrogen bonding, followed by surface complexation with metal oxides and consistent multilayer chemisorption. Furthermore, this study established a basic framework for a waste-to-remediation chain by transforming abundant and heterogeneous waste biomass into adsorbents that control AMR without any preprocessing. The findings of this study can be further extended to other broad-spectrum antibiotics present in aqueous systems. The study emphasises the need for future research on: (a) scaling up of biochar production from mixed urban green wastes for antibiotic mitigation, (b) regeneration strategies, and (c) long-term effectiveness in the natural environment.

Acknowledgements We acknowledge the Department of Science and Technology, Government of India, for the technical and financial support provided under the DST-PURSE Program (Grant No. SR/PURSE/2023/181 (G)—TPN-88132).

Author contribution All authors contributed to the conception and design of the study. Material preparation, data collection, and analysis were performed by Neenu P. Raju; data validation was conducted by Meenakshi Verma; supervision and monitoring were provided by Dr. Pooja Singh and Dr. Manikprabhu Dhanorkar. The first draft of the manuscript was written by Neenu P. Raju, and all authors commented on previous versions of the manuscript. All authors read and approved the final manuscript.

Funding This work was supported by the Department of Science and Technology, Government of India, under the DST-PURSE Program (Grant No. SR/PURSE/2023/181 (G)—TPN-88132).

Data availability All data generated or analysed during this study are included in this published article [and its supplementary information files].

Declarations

Ethics approval Not applicable.

Consent to participate Not applicable.

Consent for publication of this manuscript All authors consent to the publication of this manuscript.

Conflict of interest The authors declare no relevant financial or non-financial interests.

References

Abyaneh, M. R., Bidhendi, G. N., & Zand, A. D. (2024). Pb(II), Cd(II), and Mn(II) adsorption onto pruning-derived biochar: Physicochemical characterization, modeling and application in real landfill leachate. *Scientific Reports*. https://doi.org/10.1038/s41598-024-54028-6

Agamuthu, P., & Babel, S. (2023). Waste management developments in the last five decades: Asian perspective. *Waste Management Research*. https://doi.org/10.1177/0734242x231199938

Araújo, D., Araújo, M., Silva, S., Pereira Filho, J., Parente, M., Oliveira, R., Mazzetto, S., Oliveira, J., Edvan, R., & Bezerra, L. (2023). Effect of technical cashew nut shell liquid on growth, physicochemical and fatty acid composition of lamb meat. *Small Ruminant Research, 227*, Article 107070. https://doi.org/10.1016/j.smallrumres.2023.107070

ASTM. (2013). *Standard Practice for Proximate Analysis of Coal and Coke*. Retrieved on August 14, 2025 from https://www.astm.org/d3172-13r21e01.html

Azzam, A. M., Tokhy, Y. A., & Younes, A. A. (2022). Construction of porous biochar decorated with NiS for the removal of ciprofloxacin antibiotic from pharmaceutical wastewaters. *Journal of Water Process Engineering , 49*, 103006–103006. https://doi.org/10.1016/j.jwpe.2022.103006

Blachnio, M., Kusmierek, K., Swiatkowski, A., & Derylo-Marczewska, A. (2023). Waste-based adsorbents for the removal of phenoxyacetic herbicides from water: A comprehensive review. *Sustainability, 15*, Article 16516. https://doi.org/10.3390/su152316516

Cavali, M., Hennig, T. B., Junior, N. L., Kim, B., Garnier, V., Benbelkacem, H., Bayard, R., Woiciechowski, A. L., Matias, W. G., & Borges, A. (2025). Co-hydrothermal carbonization of sawdust and sewage sludge: Assessing the potential of the hydrochar as an adsorbent and the ecotoxicity of the process water. *Applied Science, 15*, Article 1052. https://doi.org/10.3390/app15031052

Chauhan, S., Shafi, T., Dubey, B. K., & Chowdhury, S. (2022). Biochar-mediated removal of pharmaceutical compounds from aqueous matrices via adsorption. *Waste Disposal & Sustainable Energy*. https://doi.org/10.1007/s42768-022-00118-y

Chemtai, C., Ngigi, A. N., & Kengara, F. O. (2024). Ciprofloxacin sorption by non-activated and activated biochar derived from millet husks and water hyacinth. *Sustainable Chemistry for the Environment, 5*, Article 100075. https://doi.org/10.1016/j.scenv.2024.100075

Coulibaly, A., Sako, M. K., Soro, D., Sidibé, S., & Yohan, R. (2022). Valuation of cashew nut shell for the production of biofuel. *Energy Reports, 8*, Article 691. https://doi.org/10.1016/j.egyr.2022.07.090

CPCB. (2016). *Challenges of Solid Waste Management in Urban India*. https://eacpm.gov.in/wp-content/uploads/2024/05/Solid_Waste_management_Updated.pdf

CPCB. (2025). *National Inventory on Generation and Management of Hazardous and Other Wastes (2023–24)*. Retrieved August 28, 2025 from https://cpcb.nic.in/uploads/hwmd/Annual_Inventory2022-23.pdf

Edeh, I. G., Masek, O., & Fusseis, F. (2023). 4D structural changes and pore network model of biomass during pyrolysis. *Scientific Reports*. https://doi.org/10.1038/s41598-023-49919-z

Fady, P., Richardson, A. K., Barron, L. P., Mason, A. J., Volpe, R., & Barr, M. R. (2025). Biochar filtration of drug-resistant bacteria and active pharmaceutical ingredients to combat antimicrobial resistance. *Scientific Reports, 15*(1), Article 1256. https://doi.org/10.1038/s41598-024-83825-2

Fatmawati, A., Nurtono, T., & Widjaja, A. (2023). Thermogravimetric kinetic-based computation of raw and pretreated coconut husk powder lignocellulosic composition. *Bioresource Technology Reports, 22*, Article 101500. https://doi.org/10.1016/j.biteb.2023.101500

Hadey, C., Allouch, M., Alami, M., Boukhlifi, F., & Loulidi, I. (2022). Preparation and characterization of biochars obtained from biomasses for combustible briquette applications. *The Scientific World Journal, 2022*, 1–13. https://doi.org/10.1155/2022/2554475

Haider, F. U., Wang, X., Zulfiqar, U., Farooq, M., Hussain, S., Mehmood, T., Naveed, M., Li, Y., Liqun, C., Saeed, Q., Ahmad, I., & Mustafa, A. (2022). Biochar application for remediation of organic toxic pollutants in contaminated soils; An update. *Ecotoxicology and Environmental Safety, 248*, Article 114322. https://doi.org/10.1016/j.ecoenv.2022.11432

Handiso, B., Pääkkönen, T., & Wilson, B. P. (2024). Effect of pyrolysis temperature on the physical and chemical characteristics of pine wood biochar. *Waste Management Bulletin*. https://doi.org/10.1016/j.wmb.2024.11.008

He, M., Xu, Z., Hou, D., Gao, B., Cao, X., Ok, Y. S., Rinklebe, J., Bolan, N. S., & Tsang, D. C. W. (2022). Waste-derived biochar for water pollution control and sustainable development. *Nature Reviews Earth & Environment*. https://doi.org/10.1038/s43017-022-00306-8

Islam, I. U., Qurashi, A. N., Adnan, A., et al. (2025). Bioremediation and adsorption: Strategies for managing pharmaceutical pollution in aquatic environment. *Water, Air, and Soil Pollution*. https://doi.org/10.1007/s11270-025-08193-7

Jawad, A. H., Abdulhameed, A. S., Bahrudin, N. N., Hum, N. N. M. F., Surip, S. N., Syed-Hassan, S. S. A., Yousif, E., & Sabar, S. (2021). Microporous activated carbon developed from KOH activated biomass waste: Surface mechanistic study of methylene blue dye adsorption. *Water Science and Technology, 84*, 1858–1872. https://doi.org/10.2166/wst.2021.355

Khater, E.-S., Bahnasawy, A., Hamouda, R., Sabahy, A., Abbas, W., & Morsy, O. M. (2024). Biochar production under different pyrolysis temperatures with different types of agricultural wastes. *Scientific Reports*. https://doi.org/10.1038/s41598-024-52336-5

Kumar, A., & Bhattacharya, T. (2020). Biochar: A sustainable solution. *Environment, Development and Sustainability, 23*, 6642–6680. https://doi.org/10.1007/s10668-020-00970-0

Langsdorf, A., Volkmar, M., Holtmann, D., & Ulber, R. (2021). Material utilization of green waste: A review on potential valorization methods. *Bioresources and Bioprocessing*. https://doi.org/10.1186/s40643-021-00367-5

Lewczuk, B., & Szyryńska, N. (2021). Field-emission scanning electron microscope as a tool for large-area and large-volume ultrastructural studies. *Animals, 11*, Article 3390. https://doi.org/10.3390/ani11123390

Li, J., Yu, G., Pan, L., Li, C., You, F., Xie, S., Wang, Y., Ma, J., & Shang, X. (2018). Study of ciprofloxacin removal by biochar obtained from used tea leaves. *Journal of Environmental Science, 73*, 20–30. https://doi.org/10.1016/j.jes.2017.12.024

Liu , X., Xie , Y. & Sheng, H. (2022a). Green waste characteristics and sustainable recycling options. *Research Environment Sustainability*. https://doi.org/10.1016/j.resenv.2022.10009

Liu, G., Dai, Z., Liu, X., Dahlgren, R. A., & Xu, J. (2022b). Modification of agricultural wastes to improve sorption capacities for pollutant removal from water—a review. *Carbon Research*. https://doi.org/10.1007/s44246-022-00025-1

Ma, Z., Yang, Y., Wu, Y., Xu, J., Peng, H., Liu, X., Zhang, W., & Wang, S. (2019). In-depth comparison of the physicochemical characteristics of bio-char derived from biomass pseudo components: Hemicellulose, cellulose, and lignin. *Journal of Analytical and Applied Pyrolysis, 140*, 195–204. https://doi.org/10.1016/j.jaap.2019.03.015

Mészároš, L., Šuránek, M., Melichová, Z., Frišták, V., Ďuriška, L., Kaňuchová, M., Soja, G., & Pipíška, M. (2023). Green biochar-based adsorbent for radiocesium and Cu, Ni,

and Pb removal. *Journal of Radioanalytical and Nuclear Chemistry, 332*, Article 4141. https://doi.org/10.1007/s10967-023-09104-y

Meysami, M., Rabie, A., Najafabadi, R. A., Meysami, A., & Isfahani, T. (2025). Comparative thermal and structural analysis of biochar from rapeseed meal and *Fraxinus excelsior* sawdust. *Results in Engineering, 27*, Article 106397. https://doi.org/10.1016/j.rineng.2025.106397

Mirizadeh, S., Al Arni, S., Elwaheidi, M., Salih, A. A. M., Converti, A., & Casazza, A. A. (2023). Adsorption of tetracycline and ciprofloxacin from aqueous solution on raw date palm waste. *Chemical Engineering & TechnoloGy, 46*, 1957. https://doi.org/10.1002/ceat.202300193

Murphy, O. P., Vashishtha, M., Palanisamy, P., & Kannuchamy, V. K. (2023). A review on the adsorption isotherms and design calculations for the optimization of adsorbent mass and contact time. *ACS Omega, 8*, 17407–17430. https://doi.org/10.1021/acsomega.2c08155

Naznine, F., Shafi, Z., Aafreen, U., Shahid, M., Parveen, S., & Ansari, M. I. (2025). Tracking antimicrobial resistance in river waters: Sources, key microbes, and detection techniques. *The Microbe, 7*, Article 100386. https://doi.org/10.1016/j.microb.2025.100386

Nuithitikul, K., Phromrak, R., & Saengngoen, W. (2020). Utilization of chemically treated cashew-nut shell as potential adsorbent for removal of Pb(II) ions from aqueous solution. *Scientific Reports*. https://doi.org/10.1038/s41598-020-60161-9

Panizio, R., Castro, C., Pacheco, N., Assis, A. C., Longo, A., Vilarinho, C., Teixeira, J. C., Brito, P., Gonçalves, M., & Nobre, C. (2024). Investigation of biochars derived from waste lignocellulosic biomass and insulation electric cables: A comprehensive TGA and Macro-TGA analysis. *Heliyon, 10*(18), Article e37882. https://doi.org/10.1016/j.heliyon.2024.e37882

Pusceddu, E., Santilli, S. F., Fioravanti, G., Montanaro, A., Miglietta, F., & Foscolo, P. U. (2019). Chemical-physical analysis and exfoliation of biochar-carbon matter: From agriculture soil improver to starting material for advanced nanotechnologies. *Materials Research Express, 6*, Article 115612. https://doi.org/10.1088/2053-1591/ab4ba8

Qiu, T., Li, C., Guang, M., & Zhang, Y. (2023). Porous carbon material production from microwave-assisted pyrolysis of peanut shell. *Carbon Research*. https://doi.org/10.1007/s44246-023-00079-9

Shaha, C. K., Karmaker, S., & Saha, T. K. (2024). Efficient adsorptive removal of levofloxacin using sulfonated graphene oxide: Adsorption behavior, kinetics, and thermodynamics. *Heliyon, 10*, Article e40319. https://doi.org/10.1016/j.heliyon.2024.e40319

Simonin, J. P. (2016). On the comparison of pseudo-first order and pseudo-second order rate laws in the modeling of adsorption kinetics. *Chemical Engineering Journal, 300*, Article 254. https://doi.org/10.1016/j.cej.2016.04.079

Singh, B., Camps-Arbestain, M., & Lehmann, J. (2017). *Biochar A Guide to Analytical Methods*. Csiro Publishing.

Sowjanya, B., King, P., Vangalapati, M., & Myneni, V. R. (2023). Copper-doped zinc oxide nanoparticles: Synthesis, characterization, and application for adsorptive removal of toxic azo dye. *International Journal of Chemical Engineering*. https://doi.org/10.1155/2023/8640288

Suarez, E., Tobajas, M., Mohedano, A.F., Reguera, M., Esteban, E. & de, M.A. (2023). Effect of garden and park waste hydrochar and biochar in soil application: A comparative study. *Biomass Conversion and Biorefinery.* https://doi.org/10.1007/s13399-023-04015-0

Suman, S., Panwar, D. S., & Gautam, S. (2017). Surface morphology properties of biochars obtained from different biomass waste. *Energy Sources, Part A: Recovery, Utilization, and Environmental Effects, 39*, 1007. https://doi.org/10.1080/15567036.2017.1283553

Tie, J., Shao, Y., Yan, M., & Duan, X. (2025). Cr (VI) removal by polyethyleneimine and magnetically modified garden waste biochar. *Polish Journal of Environmental Studies*. https://doi.org/10.15244/pjoes/193145

Wakejo, W. K., Meshasha, B. T., Kang, J. W., & Chebude, Y. (2022). Enhanced ciprofloxacin removal from aqueous solution using a chemically modified biochar derived from bamboo sawdust: Adsorption process optimization with response surface methodology. *Adsorption Science & Technology*. https://doi.org/10.1155/2022/2699530

Wan Mahari, W. A., Azwar, E., Foong, S. Y., Ahmed, A., Peng, W., Tabatabaei, M., et al. (2021). Valorization of municipal wastes using co-pyrolysis for green energy production, energy security, and environmental sustainability: A review. *Chemical Engineering Journal, 421*, 129749. https://doi.org/10.1016/j.cej.2021.129749

Wei, M., Shao, Y., Duan, X., & Tie, J. (2025). Polyethyleneimine-modified garden waste biochar: Preparation and its application for aqueous Cr(Ⅵ) adsorption. *Polish Journal of Environmental Studies*. https://doi.org/10.15244/pjoes/188595

Xuan, L.N. & Phuong, D. (2024). Optimizing biochar production: a review of recent progress in lignocellulosic biomass pyrolysis. *Frontiers of Agricultural Science and Engineering*. https://doi.org/10.15302/j-fase-2024597

Zafeer, M. K., & Bhat, K. S. (2023). Valorisation of agro-waste cashew nut husk (testa) for different value-added products. *Sustainable Chemistry for Climate Action*. https://doi.org/10.1016/j.scca.2023.100014

Zhang, Q., Wang, C., Cheng, J., Zhang, C., & Yao, J. (2021). Removal of Cr (VI) by biochar derived from six kinds of garden wastes: Isotherms and kinetics. *Materials, 14*, 3243–3243. https://doi.org/10.3390/ma14123243

Zhao, J., Yang, S., Bi, C., Peng, C., Wang, Y., & Tao, E. (2025). Enhanced ciprofloxacin removal from water by chitosan/Mn-modified biochar: Synergistic adsorption at multi-site active centers. *Desalination, 617*, Article 119459. https://doi.org/10.1016/j.desal.2025.119459